Numerical analysis of local head loss coefficient at the inlet of a conduit connected to a free surface channel

Van Nam Nguyen*

Hanoi Architectural University

Received 20 October 2017; accepted 28 February 2018

Abstract:

Numerical simulation have been carried out to observe and predict the mechanisms of stationary mixed flows in a free surface channel combined with a closed conduit. This study has been conducted with a wide range of discharge values, based on a free rectangular channel (4.5x0.98x0.50 m) at the upstream combined with a closed rectangular conduit (4.5 m length), located at the end of the channel. The height of the conduit is fixed at 100 mm and the conduit width is varied to form several other geometrical configurations. From the obtained numerical results, the local head losses at the transition location are computed and a relation between the local head loss coefficient at this transition and the water depth at the upstream free surface channel is proposed. It will be verified by experimental results in the next study.

Keywords: *flow contraction, mixed flows, shallow water equations.*

Classification number: *1.3*

Introduction

In most cases, when one talks about the flows, two individual kinds of flow are usually mentioned, which are the free surface flows and the pressurised flows. Free surface flows are the flows where the top flow surface is subjected to atmospheric pressure, whether the channel section is opened or closed at the top [1]. Pressurised flows are under pressure and also referred to as conduit flows or pipe flows. In practice, the simultaneous occurrence of these flow kinds is observed in many hydraulic engineering applications. Additionally, some hydraulic structures are designed to combine free surface and pressurised sections (e.g. water intakes) [2, 3]. Such flows are named "mixed flows" and have been investigated in a lot of works from both numerical and experimental point of views.

The first studies of mixed flows regimes, conducted in the decades before and after - the World War 2, were hydraulic scale models that looked at the design of particular structures. Recently, many authors have tried to establish generally applicable laws while studying particular structures or testing simulation models; and some scale models have been built [4]. However, these studies mainly focus on cases where the one-dimensional approximation is valid. For instance, see the application of a transient mixed-flow model in the design of a combined sewer storage-conveyance system [5] or a numerical study to simulate the flow conditions in a circulating water system of a thermal plant [6, 7] that was studied to define the characteristics of the transition from pressurised flow to free surface flow in a conduit, which provided some knowledge of this transition process. Li, et al. [8] conducted an investigation on the pressure transients in the sewer system; they conducted both mathematical and experimental modelling studies. Gomez, et al. [9] carried out a study to analyse the transition from free-surface to pressure flow at both ends of a pipeline. Vasconcelos, et al. [10] conducted a study about the numerical modelling of the transition between free surface and pressurised flow in storm sewers. Erpicum, et al. [2] carried out an experimental and numerical investigation of mixed flow in a gallery; Kerger [3] considered this flow with the air/water interaction on numerical simulation point of view.

On the other hand, 2D shallow flows, where the lateral velocity is not negligible with respect to the main direction one, are also common in hydraulic engineering. They have been extensively studied and modelled for years, for example, Dewals, et al. [11] analysed experimentally, numerically and theoretically the free surface flows in several shallow rectangular basins and Dufresne, et al. [12] carried out a numerical investigation on the flow patterns in rectangular shallow reservoirs. Such flows in mixed configurations, first mentioned in Nam, et al. [13], have not been fully studied thoroughly to date, neither numerically nor experimentally, especially for the flow patterns in transition regime from free surface (in a channel) to pressurised flow (in a conduit).

With the objective of contributing to the filling of this gap, a combined numerical/experimental study has been currently undertaken at the University of Liège (Belgium). The goals of

*Email: namnv79@gmail.com

this study are to assess the accuracy of an existing numerical model in representing 2D mixed flows configurations and to set up an analytical formulation to evaluate the local loss coefficient at the transition from a free surface channel to a rectangular conduit.

This paper presents the first results of the numerical simulation study, considering stationary mixed flow taking place in a free surface channel combined with a closed conduit aligned along one of the channel banks. This study has been used to define geometrical configurations and discharge ranges to be analysed experimentally as well as to choose the positions of measurement devices. In addition, numerical results provide a first data set to define the local head loss coefficient value at the transition position.

Test configurations

Geometry

The experimental study is based on the use of a 4.5 m long rectangular channel, 0.98 m wide and 0.50 m deep at the upstream, combined with a 4.5 m long rectangular cross section closed conduit aligned with side walls of the flume. The height of the conduit has been fixed to 100 mm because of discharge range considerations. The width of the conduit has been varied depending on the configurations. In this study, four geometrical configurations have been considered, namely model A-10, model B-10, model C-10 and model D-10, corresponding to a width of the conduit of L, 3L/4, 2L/4 and L/4, respectively. The conduit is located at the bottom of the channels along the right bank for all considered configurations. The dimensions and definition of these configurations are shown in Fig. 1.

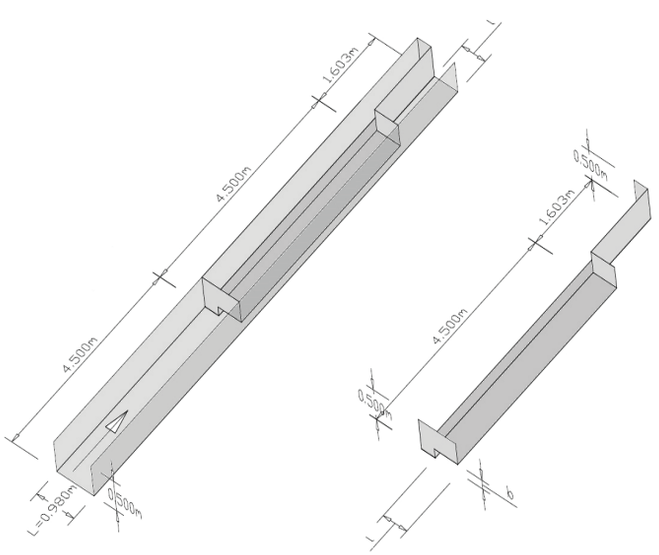

Fig. 1. Sketch of the geometrical configuration (l is the conduit width and b is the conduit height).

At the downstream, a 1.6 m long rectangular free surface channel reach has been added with a width equal to the width of the conduit in order to get a stationary downstream boundary condition and avoid a formation of a recirculation flow area, which had been discussed in Nam, et al. [13].

Hydraulic conditions

The steady discharges range was chosen depending on the geometric configuration in order to fit with the height of upstream channel walls. They are presented in the following Table 1. For the downstream water level, an example of a given discharge of 0.06 m^3/s and configuration B-10 shows a linear relation between upstream water levels and downstream ones, as presented in detail in Fig. 2.

Table 1. Characteristic and considered discharges for each geometrical configuration.

Test configurations	l (m)	b (m)	Discharge (m^3/s)
A-10	L=0.98	0.10	0.020; 0.040; 0.050; 0.060; 0.070; 0.080; 0.090
B-10	3L/4=0.735	0.10	0.010; 0.020; 0.040; 0.060; 0.080; 0.090
C-10	2L/4=0.49	0.10	0.005; 0.010; 0.020; 0.040; 0.005; 0.060; 0.080
D-10	L/4=0.245	0.10	0.005; 0.010; 0.020; 0.025; 0.030; 0.035; 0.040

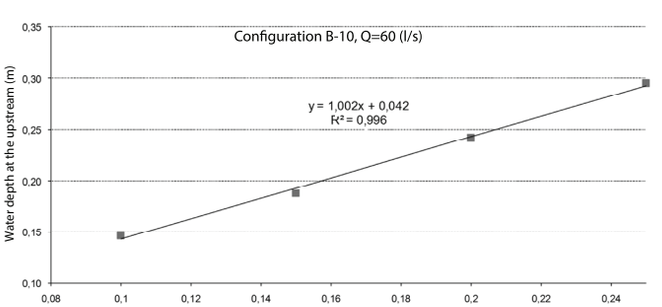

Fig. 2. Relation between upstream and downstream water depths, configuration B-10, Q = 0.06 m^3/s.

Measurement cross sections

Specific cross sections have been selected to measure flow features, in order to compute the flow energy and to compare experimental and numerical results. They are located in Fig. 3. Sections 1 and 4 are far enough from the transition section to ensure uniform flow condition and thus, to help in computing the flow energy in the free surface channel and at the closed conduit, respectively. Sections 2, 3 and section 5, 6 are characteristic of the inlet and outlet flow of the conduit, respectively. In addition, the most outlet section of the model (the section at the end of the downstream free surface channel) is used to determine the downstream boundary condition, referred as the water depth, which is fixed at 0.15 (m), whatever be the discharge and geometrical configurations.

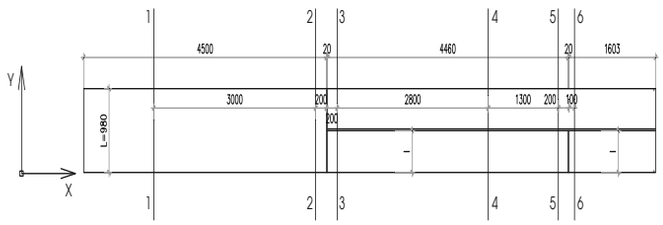

Fig. 3. Positions of the measurement cross sections - Plane view of the system.

Numerical simulations

Numerical model

The 2D multiblock flow solver WOLF2D, part of the modelling system WOLF, is based on the shallow water equations [14]. This set of equations is usually used to model two-dimensionnal unsteady open channel flows, i.e. natural flows where the vertical velocity component is small compared to both the horizontal components [15]. It is derived by depth-integrating the Navier Stoke equations. It counts for hydrostatic pressure distribution and uniform velocity components along the water depth.

Using unified pressure gradients, the shallow water equations' applicability is extended to pressurised flow. Considering the Preissmann slot model [16], pressurised flow can be calculated by the Saint-Venant equations by adding a conceptual slot on the top of a pipe. When the water depth is higer the maximum level of the cross-section pipe, it provides a free surface flow concept, for which the slot geometry affects on the gravity wave speed [3].

To deal with steady pressurised flows, the Saint Venant equations writes as in Eqs. 1-3. The Preismann slot dimensions are the mesh size as in steady flow and the pressure is not related to the slot characteristics.

$$\frac{\partial h}{\partial t}+\frac{\partial ub}{\partial x}+\frac{\partial vb}{\partial y}=0 \quad (1)$$

$$\frac{\partial}{\partial t}(bu)+\frac{\partial}{\partial x}\left(bu^2+\frac{g(2h-b)b}{2}\right)+\frac{\partial}{\partial y}(buv)=-gh_b\frac{\partial z_b}{\partial x}+gh_r\frac{\partial z_r}{\partial x}+gh_J J_x \quad (2)$$

$$\frac{\partial}{\partial t}(bv)+\frac{\partial}{\partial y}\left(bv^2+\frac{g(2h-b)b}{2}\right)+\frac{\partial}{\partial x}(buv)=-gh_b\frac{\partial z_b}{\partial y}+gh_r\frac{\partial z_r}{\partial y}+gh_J J_y \quad (3)$$

In equations 1-3, u is the velocity component along x axis, v is the velocity component along y axis, h is the water depth, b is the conduit heigth, z_b and z_r are the bottom and roof elevations, h_b, h_r, and h_J are equivalent pressure terms and J_x and J_y are the components along the axis of the energy slope. The bottom friction is conventionally modelled by the Manning formula [14]. To deal with both free surface and pressurised flows, b is computed as the minimum of the conduit elevation (infinity in case of free surface reach) and the water depth h (Fig. 4).

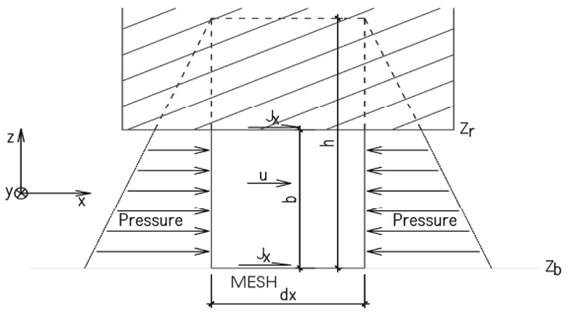

Fig. 4. Sketch of the mathematical model variables.

The conservative equations for the space discretisation was performed by tools of a finite volume scheme. This certifies a proper momentum and mass conservation, which is a requirement for handling reliably discontinuous solutions. Variable reconstruction at interfaces of cells was carried out by constant or linear extrapolation, leading to the case of a second-order spatial accuracy [15]. The flux treatment used an original flux-vector splitting technique [15]. The hydrodynamic fluxes were split and evaluated partly downstream and partly upstream according to the Von Neumann stability analysis requirements [17]. Explicit Runge-Kutta schemes were used for time integration.

Numerical computation features

Similar to many previous works of 2D shallow flows, in this study, a Cartesian grid was exploited, with a cell size of 0.01 m. Variable reconstruction at cells interfaces was performed linearly, in conjunction with slope limiting, leading to a second-order spatial accuracy [11].

Regarding the boundary conditions, the upstream boundary condition applied at the beginning of the inlet channel is the steady discharges into the model, which are presented in Table 1, and the downstream boundary condition applied at the outlet channel is generally an imposed water height of 0.15 (m) for all the considered configurations, whatever the discharge.

About the initial conditions, all the simulations were carried out starting from a channel with water at rest, having the required water depth h=0.2 (m), and in general, to ensure a convergence of the results.

Flow energy computation

Numerical simulations provide the value of water depth h (or pressure in the conduit) and the mean horizontal flow velocity components on each mesh of the computation domain. In each cross section, the mean flow energy E has been computed from this distributed result as follows:

$$E_i=\frac{\Sigma_{j=1}^{N}\left(h_j+\frac{v_j^2}{2g}\right)}{N} \quad (4)$$

where, i is the number of the cross sections (i=1÷6, see Fig. 2), N is the number of computation cells along a cross section and v_j is the velocity component of cell j, normal to the cross section.

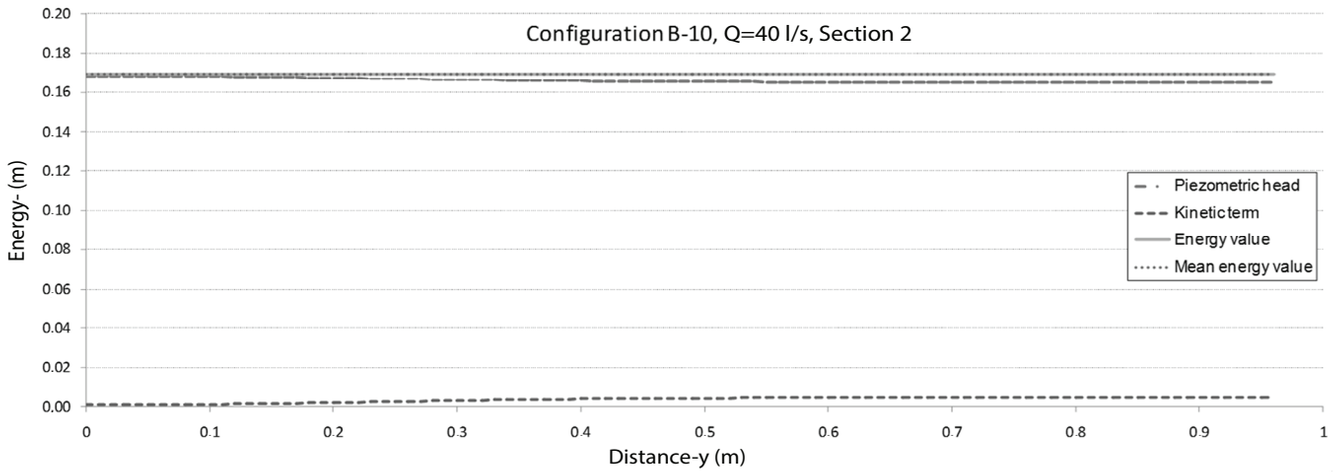

Fig. 5. Example of mean energy computation diagram of configuration B-10, Q= 40 l/s, and cross section 2.

Additionally, the mean energy computation is presented through a typical example of the geometrical configuration B-10, discharge value of 40 l/s at the cross section 2 on Fig. 5.

To evaluate the characteristics of flows at the transition position (at the conduit inlet), the local head loss due to the change of flow regimes and geometrical configurations has to be considered. From E_i values and assuming an uniform flow at the sections 1 and 4 on Fig. 2, the energy loss at this transition location (ΔE_T) is simply computed as:

$$\Delta E_T = \Delta E_{1\text{-}4} - \Delta E_{1\text{-}c} - \Delta E_{c\text{-}4} \quad (5)$$

where, $\Delta E_{1\text{-}4}$ is the total energy loss from section 1 to section 4. $\Delta E_{1\text{-}c}$, is the energy loss between section 1 and the section of the conduit inlet, $\Delta E_{c\text{-}4}$ is the energy loss between the section of the conduit inlet and section 4 (on Fig. 3). The friction resistances, which are computed according to the Manning's friction law with the uniform flow for both free surface channel and closed conduit reaches, are shown below in the following expressions:

$$\Delta E_{1\text{-}c/c\text{-}4} = J_{1\text{-}c/c\text{-}4} * l_{1\text{-}c/c\text{-}4} \quad (6)$$

$$J_{1\text{-}c/c\text{-}4} = \frac{(n v_{1\text{-}c/c\text{-}4})^2}{R_{1\text{-}c/c\text{-}4}^{4/3}} \quad (7)$$

$J_{1\text{-}c/c\text{-}4}$ are the energy slopes at the free surface channel and the conduit reaches; $v_{1\text{-}c/c\text{-}4}$ and $R_{1\text{-}c/c\text{-}4}$ are the uniform velocity and hydraulic radius at these portions, respectively; n is the Manning coefficient.

From ΔE_T values obtained in equation 5 and using the well-known formula for the local head loss computation, the head loss coefficient (k) at the transition location is computed following equation 8. It is important to correctly define the velocity (v). Particularly, all basic quantities are selected such that no problems occurr on its determination. Frequently, v is the nominal velocity, for example, the mean value of the incoming or the outgoing velocities being investigated [18]. In this investigation, v-values are related to the upstream cross section of the transition, whatever be the discharge and geometrical configurations [13].

$$k = \frac{2g\ E_T}{v^2} \quad (8)$$

Results and discussion

Energy distribution

For a given discharge and geometrical configuration, the flow energy evolution along the system can be evaluated directly from the distribution of corresponding velocity and pressure (or water depth) values on selected cross sections. The energy distribution is featured by a profile of energy value along the channel and is represented in Figs. 6-7. Fig. 6 shows the results for configuration A-10, which has the maximum conduit width (l is equal L=0.98 m) while Fig. 7 shows the results of configuration D-10, which has the minimum conduit width (l is equal L/4=0.245 m) and smaller discharge values.

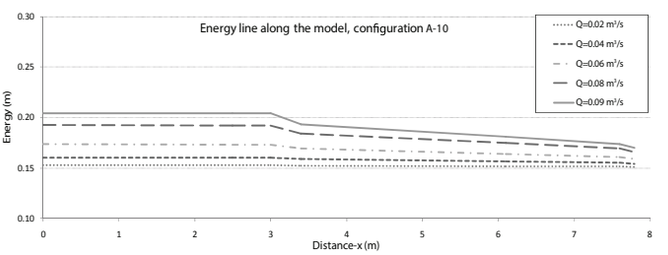

Fig. 6. Energy versus distance along the channel (sections 1-6 on Fig. 3), configuration A-10, Q=0.02-0.09 (m³/s).

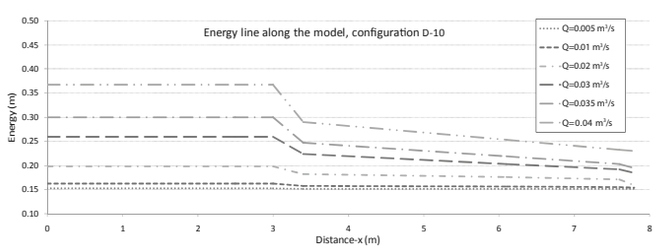

Fig. 7. Energy versus distance along the channel (sections 1-6 on Fig. 3), configuration D-10, Q=0.005-0.04 (m³/s).

These results show that, in general, the global head loss from upstream to downstream of the model is well reproduced. Additionally, it is easy to observe that the head losses are induced mainly at the conduit inlet and along the conduit while the head loss at the upstream free surface channel is much smaller. Moreover, the head loss is shown properly for the high discharge values (Q>0.03 m^3/s) and smaller conduit width; and not so clearly for smaller discharges (Q<0.02 m^3/s).

Local head loss and local head loss coefficient

Wherever the streamlines direct away from the axial direction of flow due to either a change in the wall geometry, a local head loss occurrs [17]. Additionally, for the mixed flows, the local head loss takes into account the change of the flow regimes. The final results of these values are summarised and represented in Fig. 8 for all considered configurations. These results prove that the areas ratio is the most important parameter to induce head losses, a higher head loss corresponding with a smaller conduit width value, for example, the result of configuration D-10 in Fig. 8. This can be explained by a 2D flow effect and some recirculation areas at both the top and the left side wall of the conduit. In addition, it is clearly realised that the local head loss increased following the increase in the discharge values, and thus, the flow velocity inside the conduit for each configuration.

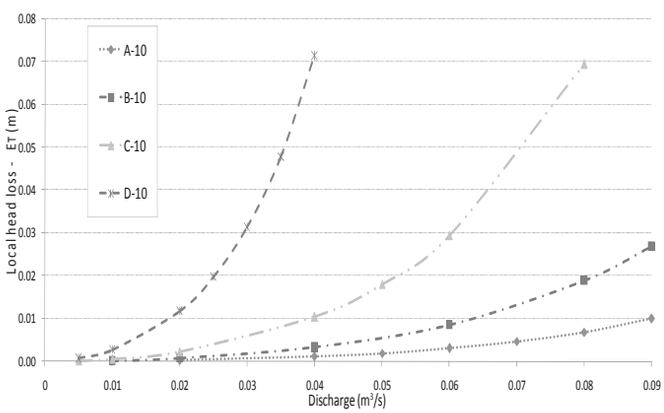

Fig. 8. Local head loss (at the transition location) versus the considered discharges for four configurations.

Regarding the local head loss coefficient (*k*), depending on the basic formula such as Gardel [19] and Idel'cik [20] to compute this *k*-value, it is only related with the referent cross sections (in case of flow contraction or expansion). In this study, from the obtained numerical results of k-values and the values of wetted areas at the cross sections 2 and 3 for whatever the discharge and all the configuration, a relation between *k*-value and such sections is proposed, and expressed as follows:

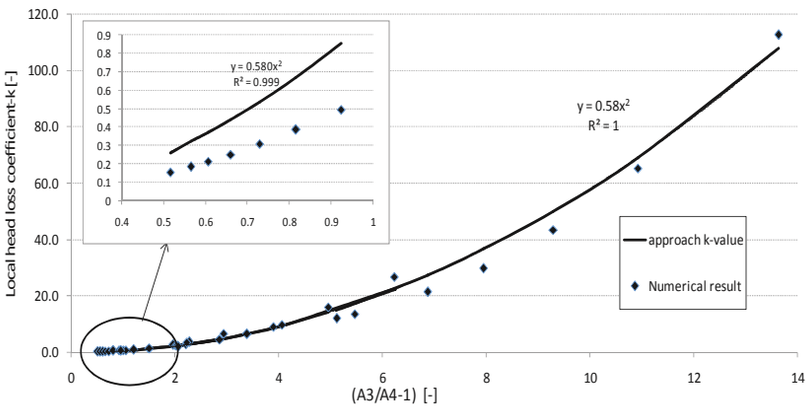

Fig. 9. Determination of the local head loss coefficient at the transition location, depending on the ratio between upstream and downstream cross section areas (at the free surface channel and the closed conduit, respectively).

$$k = 0.58*(A_2/A_3-1)^2 \quad (9)$$

where, A_2 and A_3 are the wetted areas at the cross sections 2 and 3 (in the Fig. 3), respectively.

Figure 9 shows that the k-values are in extremely good accordance with equation 9 for all the ranges of the given discharge, except configuration A-10, which is considered to have 1D flow and small k-values.

Conclusions

Several numerical simulations have been carried out to observe the flow patterns of stationary mixed flows in a free surface channel combined with a rectangular conduit of variable width. Several configurations and a wide range of discharges have been carefully considered to simulate and determine the physical parameters, providing a large set of data to characterise the flow.

The numerical results provide a first data set to define the local head loss coefficient value at the transition position and help in defining the geometrical configurations and discharge ranges to be analysed experimentally as well as to choose the positions of measurement devices.

In the next steps, an experimental study will be carried out for the same geometrical configuration to verify the numerical results, especially for the proposed formula of the local head loss coefficient at the transition position, and a detailed analysis of both physical and numerical results will be performed in order to identify the possible causes of discrepancy. In addition, similar works will be conducted for other conduit geometries to enlarge the importance of 2D effects and thus,

the complexity of the flow.

Notations:

A_2: wetted area of cross section 2

A_3: wetted area of cross section 3

B: conduit height

G: gravity acceleration

H: water depth

h_b, h_r, h_J : equivalent pressure terms

i: number of the cross section

J_x: component along the x axis of energy slope

J_y: component along the y axis of energy slope

$J_{1\text{-}c}$: energy slope at free surface channel portion from section 1 to the conduit inlet section

$J_{c\text{-}4}$: energy slope at closed conduit reach from the conduit inlet section to section 4

k : local head loss coefficient

L: upstream channel width

L: conduit width

$l_{1\text{-}c}$: length of free surface channel from section 1 to the conduit inlet section

$l_{c\text{-}4}$: length of the conduit reach from the conduit inlet section to section 4N: number of computation cells along a cross section

N: manning coefficient

$R_{1\text{-}c}$: hydraulic radial of the upstream free surface channel

$R_{c\text{-}4}$: hydraulic radial of closed conduit portion

U: velocity component along x axis

V: velocity component along y axis

v_j: velocity component of cell j normal to the cross section

x, y: space coordinate termsz_b: elevation of conduit bottom

z_r: elevation of conduit roof

ΔE_T: energy loss at the transition

$\Delta E_{1\text{-}c}$: energy loss from section 1 to the conduit inlet section

$\Delta E_{c\text{-}4}$: energy loss from the conduit inlet section to section 4

REFERENCES

[1] H. Chaudhry (2011), "Modeling of one-dimensional, unsteady, free-surface, and pressurized flows", *Journal of Hydraulic Engineering,* **137(2)**, p.10.

[2] S. Erpicum, F. Kerger, P. Archambeau, B.J. Dewals and M. Pirotton (2008), "Experimental and numerical investigation of mixed flow in a gallery", *Engineering Sciences, Computational Methods in Multiphase Flow*, **V1**.

[3] F. Kerger (2009), "Numerical simulation of 1D mixed flow with air/water interaction", *Engineering Sciences, Computational Methods in Multiphase Flow,* **V1**, p.12.

[4] S. Djordjevic and G.A. Walters (2004), "Mixed free-surface/pressurized flows in sewers", *WaPUG Meting from Scotland and Northern Ireland,* Dunblane.

[5] C. Song, J. Cardle, G.C. McDonalds, and A. Deyoung (1982), "Application of a transient mixed-flow model to the design of a combined sewer storage-conveyance system", *International Symposium on Urban Hydrology, Hydraulics and Sediment Control*, University of Kentucky.

[6] M.J. Sundquist and C.N. Papadakis (1982), "Surging in combined free surface-pressurized systems", *Journal of Transportation Engineering*, **109(2)**, pp.232-245.

[7] J.S. Montes (1997), "Transition to a free-surface flow at end of a horizontal conduit", *Journal of Hydraulic Research*, **35(2)**, p.17.

[8] J. Li and A. McCorquodale (1999), "Modeling mixed flow in storm sewers", *Journal of Hydraulic Engineering*, **125(11)**, pp.1170-1180.

[9] M. Gomez and V. Achiaga (2001), "Mixed flow modelling produced by pressure fronts from upstream and dowstream extremes", *Urban Drainage Modeling,* pp.461-470.

[10] J. Vasconcelos and S. Wright (2003), "Numerical modeling of the transition between free surface and pressurized flow in storm sewers", *Innovative Modeling of Urban Water Systems,* Monograph 12. J.W. Ontario, Canada.

[11] B.J. Dewals, S.A. Kantoush, S. Erpicum, M. Pirotton, and A.J. Schleiss (2008), "Experimental and numerical analysis of flow instabilities in rectangular shallow basins", *Environmental Fluid Mechanics,* **8**, pp.31-54.

[12] M. Dufresne, B.J. dewals, S. Erpicum, P. Archambeau and M. Pirotton (2011), "Numerical: investigation of flow patterns in rectangular shallow reservoirs", *Engineering Applications of Computational Fluid Mechanics*, **5**, pp. 247-258.

[13] N.V. Nam, S. Erpicum, B. Dewals, M. Pirroton, and P. Archambeau (2012), "Experimental investigations of 2D stationarys mixed flows and numerical comparison", *2nd IAHR Europe Congress*, Munich, Germany.

[14] S. Erpicum, T. Meile, B.J. Dewals, M. Pirotton, and A.J. Schleiss (2009), "2D numerical flow modeling in a macro-rough channel", *The International Journal for Numerical Methods in Fluids,* **61**, pp.1227-1246.

[15] S. Erpicum (2010a), "Dam-break flow computaion based on an efficient flux-vector splitting", *Journal of Computational and Applied Mathematics*, **234**, p.8.

[16] A. Preismann (1961), *Propagation des intumescences dans les canaux et rivieres in First Congress of the French Association for Computation*, Grenoble, France.

[17] S. Erpicum (2010b), "Detailed inundation modelling using high resolution DEMs", *Engineering Applications of Computational Fluid Mechanics,* **4(2)**, p.12.

[18] W.H. Hager, Ed. (2008), *Wastewater Hydraulics: Theory and Practice.*

[19] A. Gardel (1962), "Perte de charge dans un étranglement conique", *Bulletin Technique de la Suisse Romande*, **88(22)**, pp.325-337.

[20] I.E. Idel'cik, Ed. (1986), *Handbook of Hydraulic Resistance Hemisphere,* Publishing Corporation: Washington.